Appl Phys B (2009) 94: 527–533
DOI 10.1007/s00340-008-3233-x

Applied Physics B
Lasers and Optics

Trace gas sensor based on quartz tuning fork enhanced laser photoacoustic spectroscopy

K. Liu · J. Li · L. Wang · T. Tan · W. Zhang · X. Gao · W. Chen · F.K. Tittel

Received: 28 August 2008 / Published online: 11 October 2008

Abstract A compact photoacoustic gas sensor based on a quartz tuning fork and fiber-coupled distributed feedback (DFB) diode laser for detection of trace gas at atmospheric pressure has been developed. The sensor performance was evaluated by detection of water vapor in ambient air at normal atmospheric pressure. A normalized noise equivalent absorption coefficient of 1.68×10^{-8} cm^{-1} W/Hz$^{1/2}$ was achieved. Influence of different acoustic microresonators and sample pressure on the sensor performance, and the characterization of the sensor response time were investigated. Approaches to improve the current sensor performance are discussed.

PACS 42.55.Px · 42.62.Fi · 43.35.Sx

1 Introduction

Laser photoacoustic spectroscopy (PAS) is widely used in trace gas sensing applications, which is capable of a wide dynamic range, simplicity of use, high selectivity and sensitivity [1–5]. Photoacoustic spectroscopy is based on the photoacoustic effect which was first discovered by Alexander Graham Bell in 1880 [6]. When light is absorbed by a sample, the absorbed energy is transformed to heat energy by non-radiative processes, which results in an increase of the localized temperature and pressure in the sample. Therefore the absorption of modulated radiation in a sample results in the generation of an acoustic wave. The acoustic wave can be detected by using a sensitive microphone. The intensity of an acoustic signal generated by photoacoustic effect is proportional to the incident light power, absorbing sample concentration and the absorption coefficient of the target analyte.

A common approach to detect photoacoustic signal in traditional PAS is to use a resonant acoustic cell with a sensitive microphone [1, 2, 7–9]. Such a PAS detection scheme can be affected by environmental and sample gas flow noise since a microphone is designed for a widely flat frequency response. In addition, the resonant acoustic cell can not be made too small because of the resonance condition for an acoustic wave. As an alternative to microphone-based PAS, two types of novel PAS sensors based on either a cantilever or quartz tuning fork (QTF) have been recently reported. In the case of cantilever based PAS, either a miniature silicon or micromechanical cantilever is used as an acoustic transducer. The displacement of the cantilever is measured with a compact Michelson laser interferometer [10–13]. Cantilever-based PAS has demonstrated a higher detection sensitivity than that of traditional PAS: a detection sensitivity of 1.4×10^{-10} cm^{-1} W/Hz$^{1/2}$ was reported [11]. The use of a Michelson type laser interferometer makes the system more complex. In addition, the cantilever approach is also affected by environmental and sample gas flow noise as is the case of traditional PAS. The second technique is a

K. Liu · J. Li · L. Wang · T. Tan · W. Zhang · X. Gao (✉)
Environmental Spectroscopy Laboratory, Anhui Institute of Optics & Fine Mechanics, Chinese Academy of Sciences, Hefei, 230031, People Republic of China
e-mail: xmgao@aiofm.ac.cn
Fax: +86-551-5591560

W. Chen
Laboratoire de Physicochimie de l'Atmosphère, CNRS UMR 8101, Université du Littoral Côte d'Opale, 189A, Av. Maurice Schumann, 59140 Dunkerque, France

F.K. Tittel
Rice Quantum Institute, MS 366, Rice University, 6100 Main St., Houston, TX 77005, USA

QTF based PAS (QEPAS) sensor, first reported in Ref. [14]. QEPAS enables a novel way to detect a photoacoustic signal, with several useful merits including the ability to detect and quantify trace species in extremely small gas samples (few cubic millimeters) as well as immunity to ambient acoustic noise. In QEPAS, a low cost commercially available mm sized QTF with an extremely high Q factor (>10,000 at atmospheric pressure) and a resonant frequency of ~32.76 kHz is usually used as an acoustic transducer. In QEPAS the acoustic energy is accumulated in the sharply resonant QTF [14, 15], and not in a large acoustic cell as in traditional PAS. Such an approach removes the restrictions imposed on the gas cell size by the acoustic resonance conditions since the resonant frequency is now determined by the QTF. The gas enclosure is optional in QEPAS and serves only to separate the gas sample from the environment and allows control of its pressure. Owing to their excellent resonant and piezoelectric parameters, QTFs are also widely used as shear force detectors for near-field scanning, atomic force and magnetic force microscope applications, and their properties have been analyzed in detail [16–18]. With a detection sensitivity comparable to that obtained with traditional microphone-based PAS, QEPAS has been successfully applied to trace gas detection of a large number of molecules for various applications [19–24].

Analogous to conventional PAS, the photoacoustic signal intensity in QEPAS can be described as [2, 5, 15]

$$S = C\frac{\alpha P Q}{f_c}, \tag{1}$$

where C is constant, α is the absorption coefficient of the target species, P is the optical power, Q is the quality factor of the QTF, typically ranging from 10^4 to 10^5, depending on the gas pressure, and f_c is the resonant frequency of the QTF.

In order to satisfy various applications, the sensor system developed in the present work is designed to be operated in three modes: wavelength scan mode, frequency locked mode and modulation frequency scan mode.

1. Wavelength scan mode: In this mode the diode laser current modulated at half the QTF resonant frequency f_c is slowly tuned so that the laser wavelength is swept over the desired spectral range to acquire the absorption line of the molecular target.
2. Frequency locking mode. The laser wavelength is locked to the absorption line center of target species, and the modulation frequency is set to the optimum modulation frequency. This mode is very convenient for continuous on-line concentration monitoring.
3. Modulation frequency scan mode: In this case, the laser current is set to the laser wavelength at the absorption line center of the target species, and the modulation frequency is slowly tuned to sweep over the desired frequency range. In this way, we can obtain the optimum modulation frequency, the width of the QTF resonance curve and the Q factor of the QTF.

The operating mode can be controlled by a LABWINDOWS/CVI 7.0-based user interface. As an example, Fig. 1 depicts a segment of H_2O absorption spectrum at ~1.396 μm

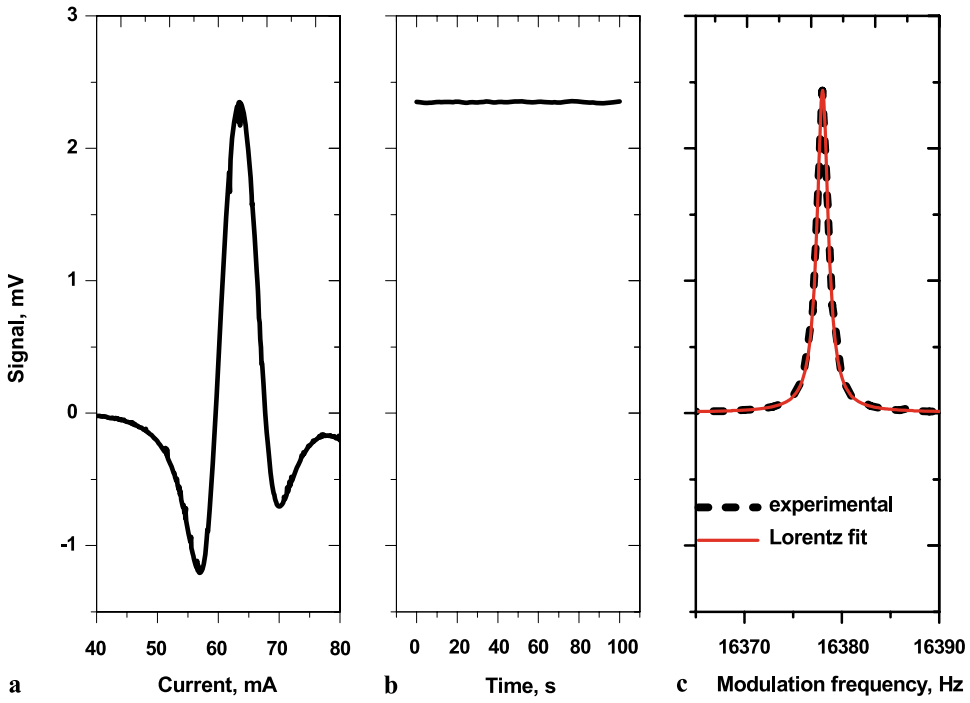

Fig. 1 QEPAS spectra of H_2O vapor in air (650 Torr pressure) recorded in three operating modes, respectively: (**a**) Wavelength scan mode: the diode laser current modulated at half the QTF resonant frequency f_c is slowly tuned to sweep over the desired spectral range. (**b**) Frequency locking mode: the diode laser current modulated at half the QTF resonant frequency f_c is locked to the absorption line peak and (**c**) Modulation frequency scan mode: the diode laser current is locked to the absorption line center, and the modulation frequency is slowly changed

that was recorded by means of the three different operation modes, respectively.

2 Sensor configuration

A schematic diagram of the QEPAS-based gas sensor platform is depicted in Fig. 2. A fiber-coupled distributed feedback (DFB) diode laser (NLK1E5GAAA, NEL JAPAN) operating at 1.396 μm and near room temperature, was used as the excitation light source for generating the photoacoustic signal. The diode laser current and temperature were controlled by a commercial diode laser controller (ILX Lightwave LDC-3724). Coarse wavelength tuning of the diode laser was achieved by changing the diode laser temperature. Fine wavelength tuning was obtained by changing the drive current or scanning the drive current of the diode laser with a ramp voltage from a function generator. The laser beam was collimated and subsequently focused between the QTF prongs by use of a lens L with a 30 mm focal length. A QTF as described in Sect. 1 was used as a photoacoustic signal transducer. The design of the QEPAS cell is depicted in Fig. 3, which equipped with two windows with 15 mm inner diameter and two gas throughputs. The length between two windows is 40 mm. In the present work, no effort was made toward miniaturizing the QEPAS cell at this stage, so the overall system can be made significantly smaller. An acoustic microresonator consisting of two stainless steel tubes, each 2.4 mm long and 0.5 mm inner diameter, was aligned perpendicular to the QTF plane to enhance the sensitivity of the sensor [14], as shown in Fig. 3. The effective resonator length was made to be equal to half of the sound wavelength ($\lambda/2 \approx 5.3$ mm in ambient air) at f_c to satisfy the acoustic resonance condition [2].

The sensor system was designed to operate in a wavelength modulation mode, which can effectively suppress the background noise originating from spectrally nonselective

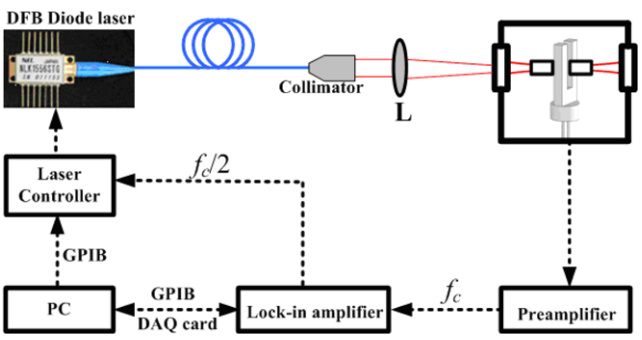

Fig. 2 Schematic of the QEPAS-based sensor platform using a fiber-coupled DFB diode laser as an excitation source. L: focusing lens, *PC*: personal computer with data acquisition card and GPIB card. The fiber-coupled DFB diode laser current is modulated at half the QTF resonant frequency f_c

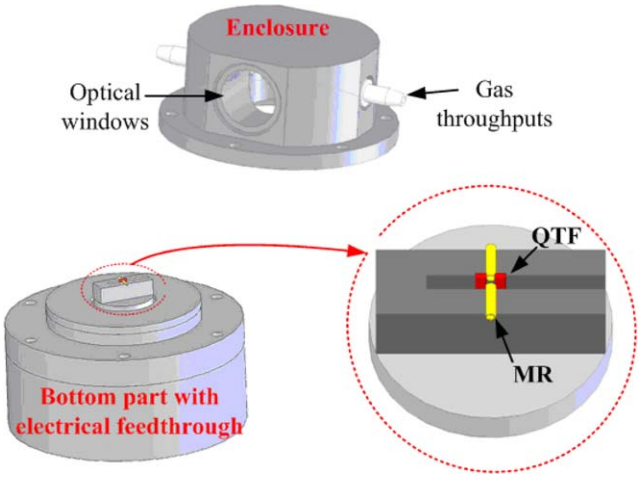

Fig. 3 Sketch of the QEPAS cell. *QTF*: quartz tuning fork; *MR*: microresonator

absorbers (such as QTF electrodes and the windows of the QEPAS gas cell). The laser current was sinusoidally modulated at half the QTF resonant frequency $f_c/2$ by a sinusoidal signal from the "SINE OUT" of a lock-in amplifier (Stanford Research Systems, Model SR 830 DSP). The QTF generated piezoelectric current was converted into a voltage using a transimpedance amplifier with a feedback resistor $R = 10$ MΩ. Subsequently, the QTF signal was amplified by a preamplifier (EG&G, Model 5113) prior to demodulation at f_c by the lock-in amplifier. The lock-in amplifier and diode laser current driver were controlled by a personal computer with a GPIB card. The second harmonic signal was acquired by an AD card and sent to the same personal computer for further analysis. All of these functions were performed with a software program based on LABWINDOWS/CVI 7.0.

3 QEPAS-based sensor characterization

3.1 Microresonator

Most studies reported to date on the QEPAS technique were performed by adding a microresonator to enhance the QEPAS signal [14, 15, 19–22]. The microresonator consists of two tubes, such as stainless steel tube, glass tube or silica tube, with inner diameter of 0.3 to 0.5 mm [14, 15, 19–22]. The effective resonant length (overall length of the two tubes plus the two gaps between the tubes and the QTF) was set to half the wavelength of sound in air at the resonant QTF frequency f_c, in order to satisfy the resonance condition. In our work, two type of microresonator were investigated. One was consisted of two aluminum tubes with a 1 mm inner diameter (referred to as MR1); the other consisted of two stainless steel tubes with a 0.5 mm inner diameter (referred to as MR2). The length of each tube was

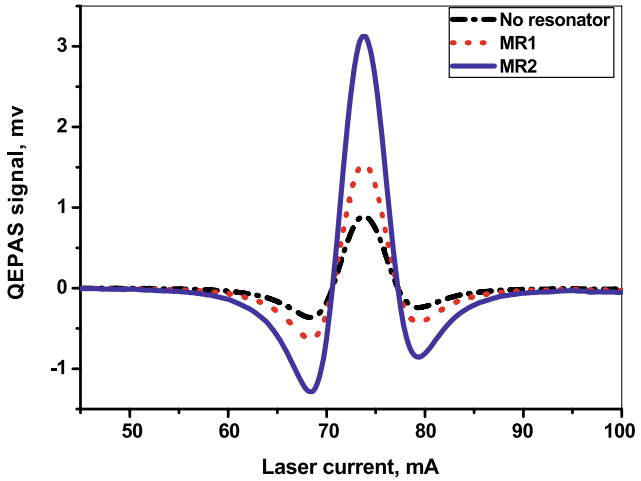

Fig. 4 Comparison of H_2O QEPAS signal acquired with and without microresonator, respectively. *MR1*: microresonator consisted of two aluminum tubes with a 1 mm inner diameter, *MR2*: microresonator consisted of two stainless steel tubes with a 0.5 mm inner diameter. The selected H_2O absorption line is 7161.41 cm^{-1} with a line intensity of 1.174×10^{-20} $cm^{-1}/(mol\,cm^{-2})$

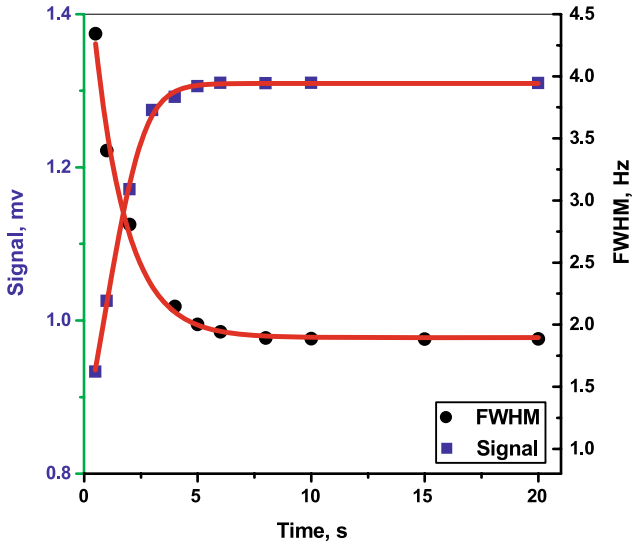

Fig. 5 Dependence of the QEPAS signal and FWHM of the QTF resonance curve measured in the modulation frequency scan mode as a function of response time

2.4 ± 0.1 mm. The overall resonant length of the microresonator was 5.4 ± 0.1 mm. The approach of installing the microresonator is schematically shown in Fig. 3. Experimentally, we found that the microresonator MR2 is better than the microresonator MR1, as shown in Fig. 4. Finally, the microresonator MR2 was selected, which enhanced the QEPAS signal by a factor of ~3. All following experimental measurements were performed with the microresonator MR2 enhanced QEPAS configuration.

3.2 Sensor response time

The response time for a QEPAS-based sensor is determined by QTF. For QEPAS, the energy is accumulated in the sharply resonant QTF, and the signal is proportional to the effective integration time $t = Q/f_c$ [14]. For commonly commercially available QTF with a typical resonant frequency of ~32.76 kHz (exactly, 32762.65 Hz in vacuum and 32754.87 Hz at normal atmospheric pressure for the QTF used in the present work) and a value of $Q \approx 10{,}000$ at normal atmospheric pressure, the corresponding energy accumulation time is $t \geq 300$ ms at lower pressures. Therefore the response time of the QEPAS-based sensor is limited to ~1 s. In our performance evaluation, the diode laser current was scanned at a rate of 2 Hz and in steps of 0.1 mA in the wavelength scan mode. However, if the sensor operates in the modulation frequency scan mode, it takes 6 to 8 s to reach full response, as shown in Fig. 5. Thus, the response time was set to 10 s when the measurements performed with the modulation frequency scan mode. This long response time is much larger than that in the wavelength scan mode. The modulation frequency scan mode is useful for a determination of the QTF characteristic parameters, while the frequency locking mode is optimum for on-line concentration monitoring.

3.3 Dependence of sample pressure on QEPAS signal

The sample pressure is an important operational parameter for quantitative detection of trace gases. In fact, the resonant frequency and the Q factor of the QTF vary significantly with pressure. Thus characterization of QTF at different pressures is necessary. In our work, characteristic parameters of the QTF (Q-factor, resonant frequency, width of the QTF resonance curve) were measured in the modulation frequency scan mode. The QTF parameters were determined by Lorentz fitting [18] of the measured data [see Fig. 1(c)] for different pressures. From the results of the fit, we can obtain the center value x_c and the full width at half maximum w of the curve. The QTF parameters can be deduced from the following equations:

$$f_c = 2x_c, \tag{2}$$

$$W_{\mathrm{QTF}} = 2w, \tag{3}$$

$$Q = \frac{f_c}{W_{\mathrm{QTF}}} \tag{4}$$

where f_c is the resonant frequency of the QTF, W_{QTF} is the full width at half maximum (FWHM) of the QTF response curve and Q is the quality factor.

Experimentally, the QTF resonant frequency decreases linearly with increasing gas pressure, as shown in Fig. 6.

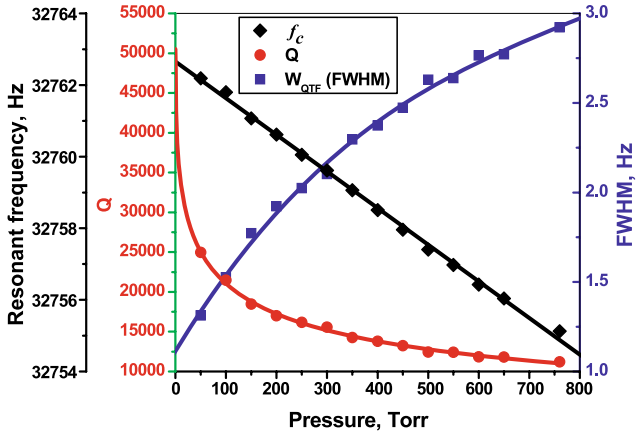

Fig. 6 Pressure dependence of the QTF characteristic parameters in the present QEPAS-based H_2O gas sensor. f_c: is the resonant frequency, Q: the quality factor, W_{QTF}: the full width at half maximum (FWHM) of the resonance curve

From a fit of the experimental results shown in Fig. 6, it is evident that the resonant frequency $f_c(p)$ can be expressed as follows:

$$f_c(p) = f_0 + kp, \tag{5}$$

where f_0 is the resonant frequency of the QTF in vacuum, p is the pressure expressed in Torr, k is a parameter specific to the QTF. We found that $k = -1.023 \times 10^{-2}$ Hz/Torr and $f_0 = 32762.65$ Hz (experimental fitted value) for the QTF used in the present work. Furthermore, the Q factor decreases significantly with increasing pressure, as show in Fig. 6. The relationship between the Q factor and the pressure can be described as follows [15]:

$$Q(p) = \frac{Q_0}{1 + Q_0 a p^b}, \tag{6}$$

where Q_0 is the Q factor value of QTF in vacuum, and a and b are the parameters specific to a particular kind of QTF. We found that for the QTF used in this work: $a = 3.286 \times 10^{-6}$, $b = 0.463$, and $Q_0 = 50{,}500$.

From Fig. 6, we observe that the Q factor of QTF decreases significantly with increasing pressure, so that the QEPAS signal decreases, as it is proportional to the Q factor of the QTF (see (1)). At the same time, the energy transfer from vibrationally excited molecules to translational degrees of freedom (V-T relaxation) by means of non-radiative processes is faster at higher pressures, resulting in more efficient acoustic excitation which yields an increase of the gas sample absorption signal with pressure. Furthermore, the use of an acoustic microresonator also changes the enhancement factor with pressure [14, 15]. These counteracting effects result in an optimum pressure at which the maximum QEPAS signal will occur. The optimum pressure depends on the targeted molecular species and the specific QTF used. In general, the optimum pressure falls in the range from 50 to 300 Torr according to results reported so far in QEPAS studies [19–23].

3.4 High noise immunity

One of the most important characteristics of QEPAS is the high immunity to ambient acoustic noise. This feature is determined by the following factors:

(a) The 1/f noise is frequency dependent and therefore it can be neglected at a relatively high resonant frequency of ~32.76 kHz.
(b) The vibration mode of the piezoelectric QTF corresponds to a symmetric vibration: the prongs move in opposite directions. This vibration mode is piezoelectrically active, while the antisymmetric vibrations resulting from environmental noise is piezoelectrically inactive [14, 15]. In other words the QTF acts like an acoustic quadrupole.
(c) The width of the QTF resonance is extremely narrow. The FWHM of the QTF resonance is ~3 Hz at normal atmospheric pressure, whereas, only 1.3 Hz at 50 Torr, as shown in Fig. 6. Therefore only the frequencies that occur in this narrow band can effectively excite a QTF response.

4 QEPAS measurements of H_2O vapor

The main objective of the present work was to develop a compact and low cost sensitive gas sensor operating at atmospheric pressure. The sensor performance was evaluated by selecting water vapor in ambient air as the target analyte. The absorption line selection for water vapor detection was made using the HITRAN04 database. An H_2O absorption line at 7165.82 cm^{-1} with a line intensity of 5.93×10^{-21} $cm^{-1}/(mol\,cm^{-2})$ was chosen as the optimum QEPAS excitation wavelength. The measurements were carried out with 0.64% H_2O vapor in ambient air, corresponding to a relative humidity of 26% at 21°C and 1 atm.

The laser power delivered to the QTF at the target wavelength was measured to be ~8 mW. The QTF signal was amplified by a gain factor of 25 with a commercial preamplifier (EG&G, Model 5113, bandpass filter = 10–100 kHz) before demodulation at f_c by use of a lock-in amplifier. The time constant of the lock-in amplifier was set to 1 s (18 dB/oct filter slope, $\Delta f = 0.19$ Hz). A spectrum of 0.64% water vapor in air, measured at atmospheric pressure is shown in Fig. 7. The noise level was determined by the standard deviation deduced from baseline measurements in a non-absorption portion of the H_2O vapor spectrum, and was found to be ~2.32 μV (1σ), which corresponds to a signal-to-noise ratio (SNR) of ~690. Thus, the normalized noise equivalent

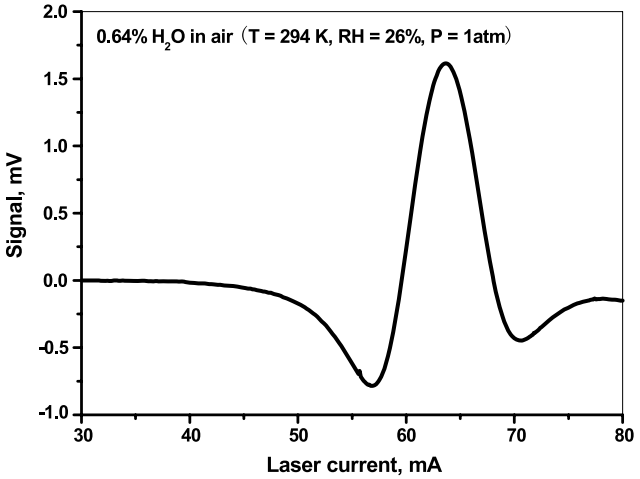

Fig. 7 QEPAS signal of 0.64% H_2O vapor ($T = 21°C$, RH = 26%) detected in ambient air at atmospheric pressure, the selected absorption line is 7165.82 cm^{-1}. Diode laser power delivered to the QTF cell is 8 mW, lock-in amplifier time constant is set at 1 s

absorption coefficient (1σ) of the QEPAS water vapor sensor is 1.68×10^{-8} cm^{-1} $W/Hz^{1/2}$ at atmospheric pressure. In the reported work, we did not consider the optimum pressure for the detection of H_2O, because our objective was to develop a QEPAS-based gas sensor operating at atmospheric pressure.

5 Conclusions

A low cost, simple to use and highly sensitive gas sensor was developed based on photoacoustic spectroscopy using a QTF in combination with a fiber-coupled DFB diode laser. The QEPAS sensor performance was evaluated by means of the detection of water vapor in ambient air with a normalized noise equivalent absorption coefficient of 1.682×10^{-8} cm^{-1} $W/Hz^{1/2}$ at normal atmospheric pressure. As the QEPAS signal intensity is proportional to the Q factor of QTF, and the Q factor increases at lower pressure, a higher detection sensitivity of $\sim 10^{-9}$ cm^{-1} $W/Hz^{1/2}$ can be obtained if the QEPAS-based sensor system operates at an optimum pressure. Kosterev et al. [25] have reported H_2O vapor detection based on QEPAS at 7306.75 cm^{-1} where the line intensity S is equal to 1.79×10^{-20} $cm^{-1}/(mol\,cm^{-2})$, about 3.3 times higher than that used in the present work. In this case, a normalized noise equivalent absorption coefficient of 1.9×10^{-9} $cm^{-1}W/Hz^{-1/2}$ was achieved at an optimum pressure of 60 Torr.

Since the QEPAS signal is laser power dependent, the detection sensitivity of the sensor can be improved by using high power laser sources, such as high power diode lasers and fiber-amplified diode lasers [26]. Because the photoacoustic signal intensity is inversely proportional to the modulation frequency (see (1)), a QTF with a lower resonant frequency ($\sim$10–15 kHz) would be desirable for sensitivity improvement. Furthermore, the use of an improved acoustic microresonator can contribute to QEPAS sensitivity enhancement by a factor of >10 depending on its design and choice of material [14, 27].

QEPAS offers several important advantages in addition to low cost, such as a high immunity to ambient acoustic noise and very small sample volume. These features can potentially lead to the development of ultra-compact portable gas sensor technology for various field applications in environmental monitoring and medical diagnostics.

Acknowledgements This research was funded by the National 863 High Technology Research and Development Program of China under Grant No. 2006AA06Z237, and in part by the French International Program of Scientific Cooperation (CNRS/PICS n°3359). The authors are grateful to Dr. Anatoliy A. Kosterev of Rice University for his helpful advice and numerous discussions.

References

1. J.S. Li, X.M. Gao, L. Fang, W.J. Zhang, H. Cha, Opt. Laser Technol. **39**, 1144 (2007)
2. A. Miklos, P. Hess, Z. Bozoki, Rev. Sci. Instrum. **72**, 1937 (2001)
3. M.G. Da Silva, H. Vargas, A. Miklos, P. Hess, Appl. Phys. B **78**, 677 (2004)
4. M.A. Gondal, Appl. Opt. **36**, 3195 (1997)
5. S. Schilt, L. Thevenaz, M. Nikles, L. Emmenegger, C. Huglin, Spectrochim. Acta A **60**, 3259 (2004)
6. A.G. Bell, Am. J. Sci. **20**, 305 (1880)
7. J.S. Li, X.M. Gao, W.Z. Li, Z.S. Cao, L.H. Deng, W.X. Zhao, M.Q. Huang, W.J. Zhang, Spectrochim. Acta A **64**, 338 (2005)
8. F.G.C. Bijnen, J. Reuss, F.J.M. Harren, Rev. Sci. Instrum. **67**, 2914 (1996)
9. A. Petzold, R. Niessner, Appl. Phys. Lett. **66**, 1285 (1995)
10. V. Koskinen, J. Fonsen, K. Roth, J. Kauppinen, Appl. Phys. B **86**, 451 (2007)
11. T. Laurila, H. Cattaneo, T. Poyhonen, V. Koskinen, J. Kauppinen, R. Hernberg, Appl. Phys. B **83**, 285 (2006)
12. K. Wilcken, J. Kauppinen, Appl. Spectrosc. **57**, 1087 (2003)
13. T. Laurila, H. Cattaneo, V. Koskinen, J. Kauppinen, R. Hernberg, Opt. Express **13**, 2453 (2005)
14. A.A. Kosterev, Y.A. Bakhirkin, R.F. Curl, F.K. Tittel, Opt. Lett. **27**, 1902 (2002)
15. A.A. Kosterev, F.K. Tittel, D.V. Serebryakov, A.L. Malinovsky, I.V. Morozov, Rev. Sci. Instrum. **76**, 043105 (2005)
16. F.J. Giessibla, Appl. Phys. Lett. **73**, 3956 (1998)
17. D.V. Serebryakov, A.P. Cherkun, B.A. Loginov, V.S. Letokhov, Rev. Sci. Instrum. **73**, 1795 (2002)
18. R.D. Grober, J. Acimovic, J. Schuck, D. Hessman, P.J. Kindlemann, J. Hespanha, A.S. Morse, K. Karrai, I. Tiemann, S. Manus, Rev. Sci. Instrum. **71**, 2776 (2000)
19. A.A. Kosterev, F.K. Tittel, Appl. Opt. **43**, 6213 (2004)
20. M. Horstjann, Y.A. Bakhirkin, A.A. Kosterev, R.F. Curl, F.K. Tittel, C.M. Wong, C.J. Hill, R.Q. Yang, Appl. Phys. B **79**, 799 (2004)
21. A.A. Kosterev, Y.A. Bakhirkin, F.K. Tittel, Appl. Phys. B **80**, 133 (2005)
22. R. Lewicki, G. Wysocki, A.A. Kosterev, F.K. Tittel, Appl. Phys. B **87**, 157 (2007)

23. G. Wysocki, A.A. Kosterev, F.K. Tittel, Appl. Phys. B **85**, 301 (2006)
24. M.D. Wojcik, M.C. Phillips, B.D. Cannon, M.S. Taubman, Appl. Phys. B **85**, 307 (2006)
25. A.A. Kosterev, F.K. Tittel, T.S. Knittel, A. Cowie, J.D. Tate, in *Laser Applications to Chemical, Security and Environmental Analysis (LACSEA)*, Incline Village, NV, February 5–9 (2006)
26. M.E. Webber, M. Pushkarsky, C.K.N. Patel, Appl. Opt. **42**, 2119 (2003)
27. A.A. Kosterev, Y.A. Bakhirkin, F.K. Tittel, S. McWhorter, B. Ashcroft, Appl. Phys. B **92**, 103 (2008)